ACS SyntheticBiology

pubs.acs.org/synthbio Research Article

Whole-Cell Biosensor and Producer Co-cultivation-Based Microfluidic Platform for Screening *Saccharopolyspora erythraea* with Hyper Erythromycin Production

Erbing Hua,[‖] Yue Zhang,*[,‖] Kaiyue Yun, Wenjia Pan, Ye Liu, Shixin Li, Yan Wang, Ran Tu,* and Meng Wang*

Cite This: *ACS Synth. Biol.* 2022, 11, 2697−2708 Read Online

ACCESS | Metrics & More | Article Recommendations | Supporting Information

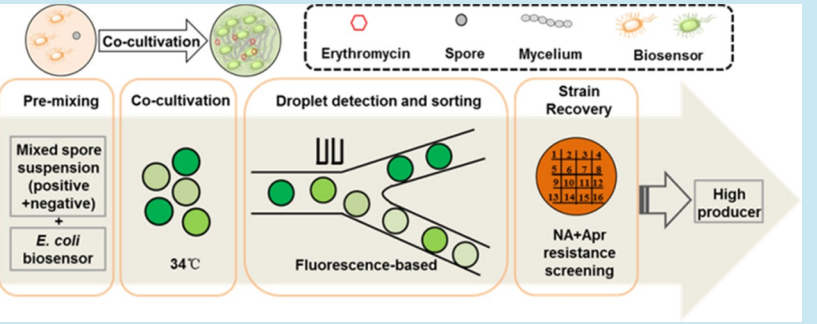

ABSTRACT: Actinomycetes are versatile secondary metabolite producers with great application potential in industries. However, industrial strain engineering has long been limited by the inefficient and labor-consuming plate/flask-based screening process, resulting in an urgent need for product-driven high-throughput screening methods for actinomycetes. Here, we combine a whole-cell biosensor and microfluidic platform to establish the whole-cell biosensor and producer co-cultivation-based microfluidic platform for screening actinomycetes (WELCOME). In WELCOME, we develop an MphR-based *Escherichia coli* whole-cell biosensor sensitive to erythromycin and co-cultivate it with *Saccharopolyspora erythraea* in droplets for high-throughput screening. Using WELCOME, we successfully screen out six erythromycin hyper-producing *S. erythraea* strains starting from an already high-producing industrial strain within 3 months, and the best one represents a 50% improved yield. WELCOME completely circumvents a major problem of industrial actinomycetes, which is usually genetic-intractable, and this method will revolutionize the field of industrial actinomycete engineering.

KEYWORDS: *whole-cell biosensor, actinomycetes, co-cultivation, droplet-based microfluidic, high-throughput screening, erythromycin*

1. INTRODUCTION

Actinomycetes are well known for their tremendous potential of producing secondary metabolites, contributing to various antimicrobial, anthelmintic, and anticancer compounds, and about two-thirds of all of the discovered antibiotics,[1] many of which are clinically important, such as erythromycin, tetracycline, and vancomycin.[2] Some strains, including *Streptomyces avermitilis*, *Streptomyces fradiae*, and *Saccharopolyspora erythraea*, are workhorses in industrial fermentation over years to produce critical antibiotics. For instance, the production of avermectin B1a from *S. avermitilis* is significantly improved 1000-fold through engineering,[3] contributing to an annual sale of more than 1 billion USD.[4] The potential in the production of sencondary metabolites makes actinomycetes important industrial strains and attracts extensive effort to improve their performances in industrial production. Random mutagenesis using UV light, chemical reagents, atmospheric and room-temperature plasma (ARTP), and heavy ion followed by screening using 24-, 48-, and 96-well microtiter plates (MTPs) or flasks is still the predominant method in the field of industrial actinomycetes engineering.[5] All strains have to be cultivated individually and assessed by a series of conventional methods such as chromatography and mass spectrometry, which are inefficient and labor-consuming, leading to the limited capability of obtaining improved variants. On the other hand, high-throughput screening (HTS) methods, such as flow cytometry, were now regularly used for engineering unicellular microorganisms, while the development of an effective and efficient HTS method for actinomycetes is still falling behind. In our

Received: February 24, 2022
Published: May 13, 2022

https://doi.org/10.1021/acssynbio.2c00102
ACS Synth. Biol. 2022, 11, 2697−2708

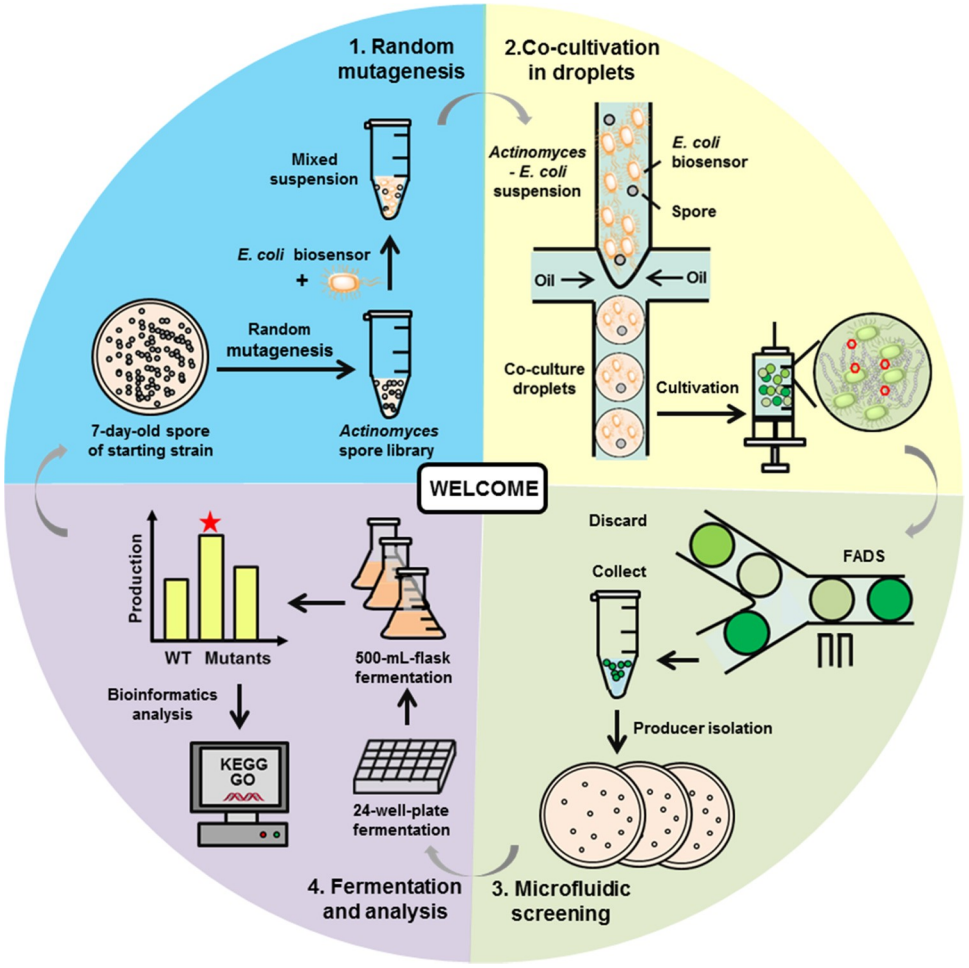

Figure 1. Workflow of WELCOME for product-driven HTS of actinomycetes. One round of product-driven screening contains four steps, including random mutagenesis, co-cultivation in droplets, microfluidic screening, and fermentation and analysis. The screened hyperproducers can be used as the starting strains for iterative rounds of mutagenesis and screening. Red hexagons in the step of "co-cultivation in droplets" represented the secondary metabolite produced by the actinomycete that served as the effector molecules of biosensors.

previous work, we have established a droplet-based microfluidic platform for high-throughput screening of *Streptomyces*.[6] *Streptomyces* spore was individually encapsulated in a 400 pL micro-bioreactor that supported a variety of physiological activities and biochemical reactions, including spore germination, protein synthesis, and secondary metabolites biosynthesis. Using this platform, expression regulatory element and target enzyme screening were successfully performed in *Streptomyces lividans* using engineered promoters and cellulase as examples. However, a droplet-based microfluidic screening method for secondary metabolites produced by actinomycetes has not been realized and is in urgent need.

Most secondary metabolites are not natural chromophores; therefore, biosensors are critical tools to facilitate the HTS processes.[7] A transcriptional factor (TF)-based biosensor is composed of a regulatory protein in response to the specific effector molecule, a promoter subjected to regulation, and a reporter gene. In a whole-cell biosensor, the intracellular concentration of the effector molecule can be translated into the expression level of the downstream reporter gene, thus conferring different viability or fluorescence intensity to the cells. Biosensor-based fluorescence-activated cell sorting (FACS) can facilitate product-driven strain engineering and HTS processes in a single-cell resolution.[8−12] *Escherichia coli* strains are the most commonly used hosts of whole-cell biosensors probably because of their clear genetic background and the easy access of extensive genetic manipulation tools.[10]

MphR is a transcription repressor belonging to the TetR family that recognizes a broad scope of macrolide molecules as its ligands.[13,14] Williams and co-workers have reported an engineered MphR-based biosensor that specifically responds to erythromycin and suggested the potential application of MphR in the HTS of macrolides.[13] In this work, we combined MphR-based whole-cell biosensor and our microfluidic platform to create the whole-cell biosensor and producer co-cultivation-based microfluidic platform for screening actinomycetes (WELCOME), which enabled the HTS of secondary metabolite hyperproducers from actinomycetes. In WELCOME, the *E. coli* biosensor strain and the erythromycin-producing strain *S. erythraea* were co-cultivated in droplets and different erythromycin production levels can be positively related to green fluorescence strength and recognized by fluorescence-activated droplet sorting (FADS). Then, *S. erythraea* strains with higher productions can be screened, recovered for traditional fermentation confirmation, and subjected to further bioinformatics analysis (Figure 1). Using WELCOME, continuous evolution of industrial strains for higher productions can be efficiently achieved through iterative mutagenesis and screening.

https://doi.org/10.1021/acssynbio.2c00102
ACS Synth. Biol. 2022, 11, 2697−2708

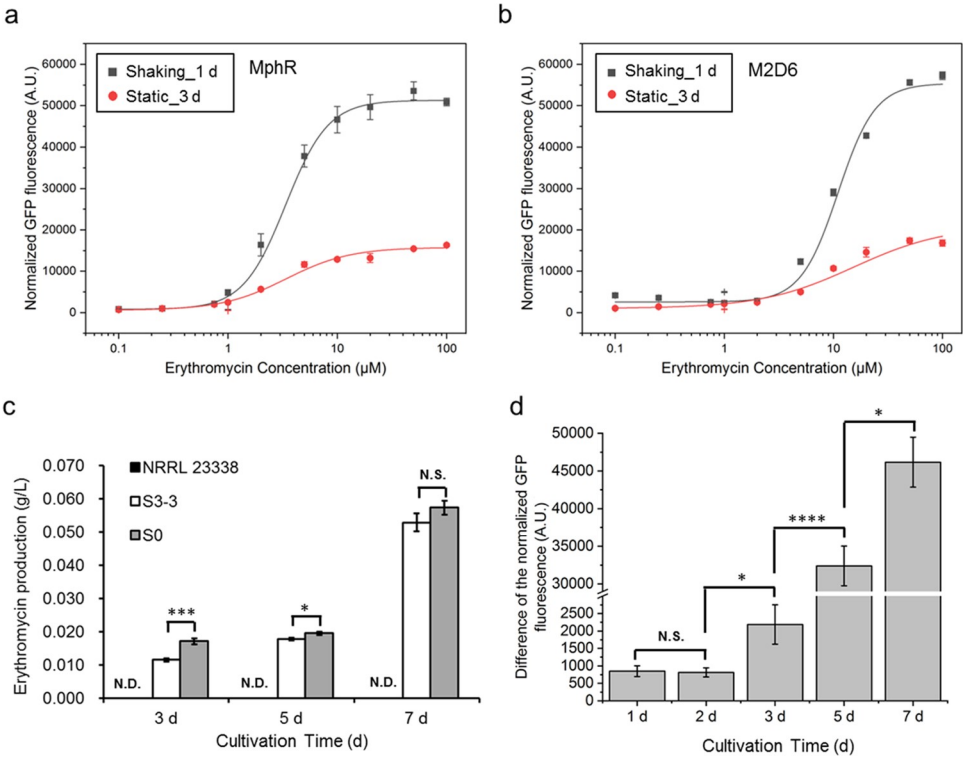

Figure 2. Function analysis of biosensor strains and erythromycin productions of different strains. Dose−response curves of *E. coli* biosensor strain Top10/MphR (a) and Top10/M2D6 (b) under the shaking condition after 1-day cultivation and under the static condition after 3-day cultivation. (c) Erythromycin productions of *S. erythraea* NRRL 23338, S3-3, and S0 in LB medium. ND represents "not detectable". (d) Difference in the normalized GFP fluorescence of S3-3 + Top10/mphR co-cultivation system (F1) and Top10/mphR culture (F2) in LB medium under the static condition. Error bars represent the standard errors of the mean ($n = 3$). *$p \leq 0.05$, ***$p \leq 0.001$, ****$p \leq 0.0001$, and NS indicated no significant difference (Student's two-tailed *t*-test).

Starting from an already high-producing industrial *S. erythraea* strain S0, we successfully screened out several mutants with higher productions through iterative ARTP random mutagenesis and HTS using this method, among which the best mutant represented 50% improved erythromycin yield compared to the starting strain. To the best of our knowledge, this is the first report describing the HTS of secondary metabolite hyperproducers from actinomycetes by FADS. Given that actinomycetes are critical producers of many important pharmaceuticals and the industry has been trapped in low-efficiency traditional screening for decades, combined with rational or semirational mutant library creation methods in actinomycetes, WELCOME would revolutionize the field of industrial actinomycete engineering.

2. RESULTS

2.1. Function Analysis of Biosensor Strains for WELCOME. According to the previous report,[13] MphR and its variant M2D6 can sense erythromycin of different concentrations. Based on this work, two dual-plasmid *E. coli* biosensor strains Top10/MphR and Top10/M2D6 harboring plasmids pMphR (carrying *mphr* gene) and pM2D6 (carrying *m2d6* gene), respectively, and sharing plasmid pMphA (carrying macrolide phosphotransferase gene *mpha*), were constructed. The biosensor strains were first cultivated in the presence of 10 μM erythromycin for 3 h were observed by a fluorescence microscope to verify if they can sense erythromycin. We observed that Top10/MphR and Top10/M2D6 showed no fluorescence when erythromycin was absent, while they reflected obvious green fluorescence when 10 μM erythromycin was added (Figure S1). This result demonstrated that two *E. coli* biosensor strains that can sense erythromycin were successfully constructed.

To characterize the properties of these two biosensor strains, Top10/MphR and Top10/M2D6 were cultivated with various erythromycin concentrations. The dose−response curves of these two biosensor strains cultivated at 34 °C, shaking condition, and 34 °C, static condition (which mimic cell growth in droplets), respectively, were determined. Generally speaking, the normalized fluorescence intensity gradually increased as the cultivation time prolonged. At the same time interval, the normalized fluorescence intensities were first increased with the increased erythromycin concentrations and then decreased when the concentration was higher than 100 μM, which might be due to the cytotoxicity caused by the high concentration of erythromycin as an antibiotic (Figure S2). Compared to the shaking condition, the fluorescence response under the static condition increased much slowly. The $K_{1/2}$ value, representing the concentration of erythromycin when half-maximum normalized GFP fluorescence was obtained, was used to evaluate the sensitivity of the biosensor. The $K_{1/2}$ value of MphR was 3.37 μM after 1-day cultivation under shaking condition, while a comparable 3.4 μM of $K_{1/2}$ value was obtained after 3-day cultivation under static condition (Figure 2a). In terms of M2D6, these two values were 11.02 μM (shaking, 1 day) and 15.30 μM (static, 3 days), respectively (Figure 2b). From the dose−response curves, we can conclude that the optimal detection ranges of MphR and M2D6 were 1−20 and 5−100 μM, respectively. These results demonstrated that MphR was more sensitive to erythromycin than M2D6 because it

https://doi.org/10.1021/acssynbio.2c00102
ACS Synth. Biol. 2022, 11, 2697−2708

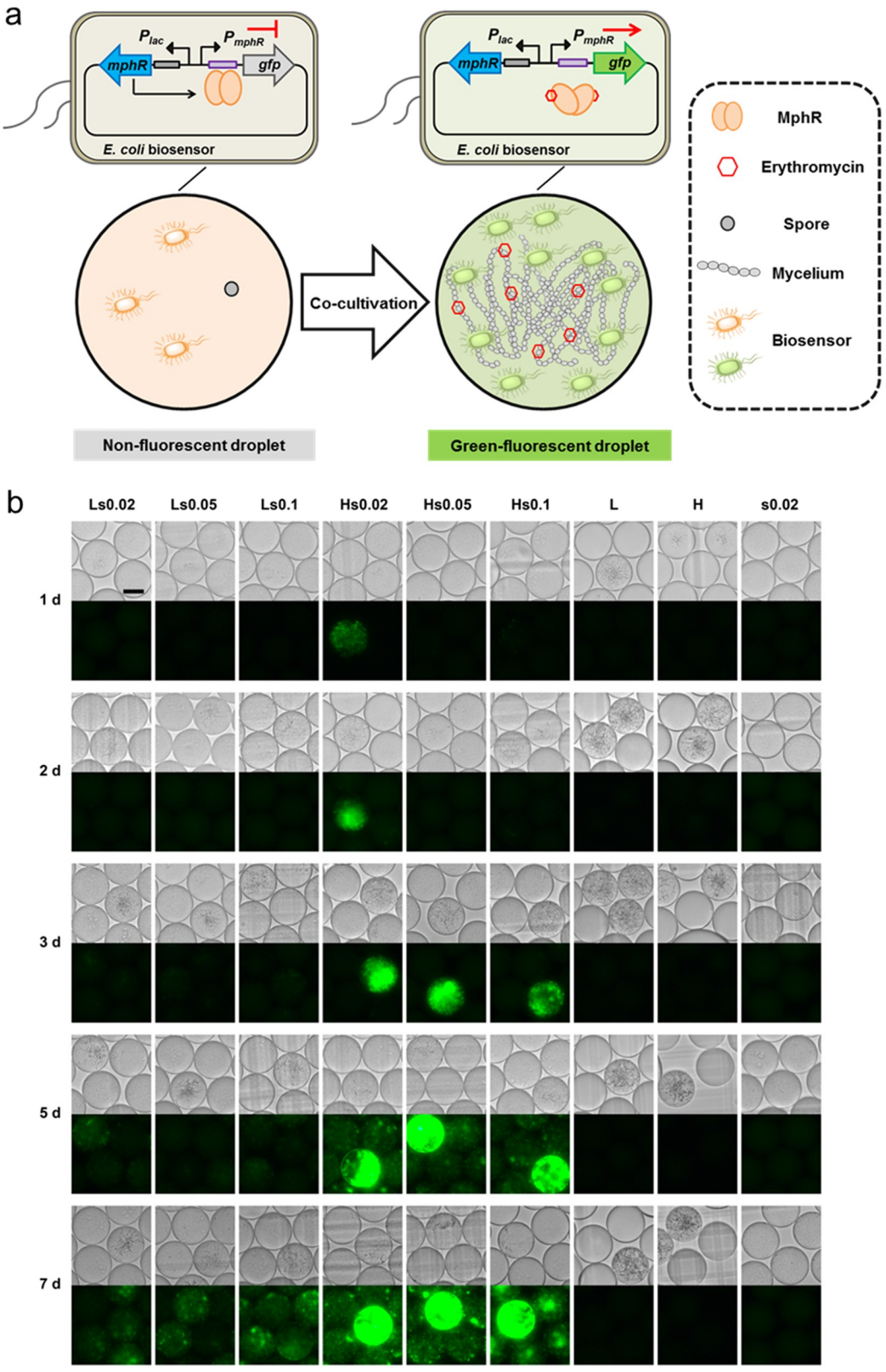

Figure 3. Development of *S. erythraea*−*E. coli* co-cultivation system in droplets. (a) Schematic diagram of the erythromycin-fluorescence response in a *S. erythraea*−*E. coli* co-cultivation droplet. In the early stage, *gfp* transcription was inhibited by the interaction of MphR protein (orange ellipses) and the promoter P_{mphR}. After a period of co-cultivation, the spore (gray dot) proliferated to mycelium (gray chain) and began to produce erythromycin (red hexagons). The erythromycin molecules that penetrate *E. coli* cells would interact with MphR protein to release *gfp* transcription, contributing green fluorescence of the co-cultivated droplets. (b) Microscopic observation of different co-cultivation droplets at different time intervals. "*H*" indicates high-production strain *S. erythraea* S3-3, "*L*" indicates low-production strain *S. erythraea* NRRL 23338, and "*s*" indicates *E. coli* biosensor strain Top10/MphR. The numbers 0.02, 0.05, and 0.1 indicate different final concentrations (OD_{600}) of *E. coli* cells in droplets. Scale bar: 50 μm.

https://doi.org/10.1021/acssynbio.2c00102
ACS Synth. Biol. 2022, 11, 2697−2708

exhibited a relatively lower $K_{1/2}$ value and a narrower detection range.

To co-encapsulate *E. coli* and *S. erythraea* in droplets, a clear fermentation medium that is compatible with FADS is needed. Starch, dextrin, and soybean powder are usually the main components of the fermentation medium for erythromycin production in the industry. However, this medium is viscous and turbid, which is not suitable for droplet generation and FADS screening. Since biosensors functioned well in LB medium, we tested whether *S. erythraea* strains can produce erythromycin in LB medium. Three erythromycin-producing *S. erythraea* strains, low-producing wild-type *S. erythraea* NRRL 23338, and industrial high-producing S0 and S3-3, were fermented in 24-well plates containing LB medium, respectively, and their erythromycin productions were measured by the modified colorimetric method on day 3, day 5, and day 7. We found that the erythromycin production of *S. erythraea* NRRL 23338 was hardly detected even when the cultivation time was prolonged to 7 days, while two high-producing strains, S3-3 and S0, produced 0.012 g/L (15.68 μM) and 0.017 g/L (23.32 μM) erythromycin after 3-day cultivation, respectively, and a similar amount of erythromycin after 7-day cultivation (Figure 2c). This result showed that *S. erythraea* strains can produce erythromycin in LB medium. Thus, the LB medium can be used to co-cultivate *S. erythraea* and biosensor strains.

Droplet-based cultivation is more similar to that under the static condition rather than the shaking condition. Before we co-encapsulated *S. erythraea* and *E. coli* in droplets, we co-cultivated them under the static condition to verify if they grew normally in a co-cultivation system and whether biosensors can respond to the erythromycin produced by the *S. erythraea* strains. The mixture of Top10/MphR cells and S3-3 spores was inoculated in a 96-well plate, where the resultant cell density (OD_{600}) of *E. coli* was 0.1 and the concentration of *S. erythraea* was 1×10^6 spore/mL. The culture containing merely S3-3 was used as the control. The differences in the normalized GFP fluorescences of S3-3 + Top10/MphR co-cultivation system (F1) and Top10/mphR culture (F2) were determined at different time intervals. We found that F1 was slightly greater than F2 since day 1, indicating that the biosensor began to respond to erythromycin at this time point. The differences in F1 and F2 were not significant within 2 days and increased sharply from day 3 to day 5, which was due to the accumulation of erythromycin in the co-cultivation system in this period (Figure 2d). This result showed that the presence of biosensors did not influence erythromycin production of *S. erythraea*, and the biosensor was functional in the *S. erythraea*−*E. coli* co-cultivation system.

2.2. Development of WELCOME for Screening Erythromycin Hyperproducers. Because pMphA and pMphR were all replicative plasmids, the *E. coli* biosensor strain Top10/MphR was usually cultivated in the antibiotic-containing LB medium. However, *S. erythraea* growth was inhibited when chloramphenicol or ampicillin was added in the medium, which renders the co-cultivation of *S. erythraea* and Top10/MphR in an antibiotic-containing LB medium impossible. If pMphA and pMphR could be stably maintained in Top10/MphR without antibiotics, which did not affect its function as a biosensor strain, then co-cultivation of *S. erythraea* and Top10/MphR would still be feasible. We cultivated Top10/MphR strain in the antibiotic-free LB medium, and 3-day-old and 7-day-old broths were diluted and applied on the antibiotic-free LB agar plates and dual-antibiotic-containing LB agar plates, respectively. The results showed that the number of the emerging colonies on two kinds of agar plates represented no significant difference after both 3-day and 7-day cultivation (Table S1), indicating that pMphA and pMphR had been well maintained within 7-day cultivation when antibiotics were absent. Thus, in the following experiments, *S. erythraea* and Top10/MphR would be co-cultivated in an antibiotic-free LB medium and the biosensor system could still function normally.

Erythromycin high-producing strain *S. erythraea* S3-3 was first used in a preliminary experiment. Seven-day-old spores were collected from the agar plate, suspended together with Top10/MphR in LB medium, and co-encapsulated in droplets. We noted that spores can germinate normally in the co-cultivation system. However, all droplets, including those that did not contain mycelium, exhibited obvious green fluorescence after 3-day cultivation. We speculated that this phenomenon was due to the erythromycin produced during *S. erythraea* growth on the agar plate, which contaminated our spore collection. To solve this problem, the collected spore suspension was repeatedly washed with LB medium and filtrated through a 10 kDa cutoff protein concentrator. In this way, the erythromycin contamination can be completely removed (Figure S3).

The initial ratio of *S. erythraea* spores and *E. coli* cells is a key factor in the co-cultivation system. More biosensor cells mean a stronger fluorescence response to erythromycin, while excess *E. coli* cells will compete more intensely for the limited carbon source, nitrogen source, and living space with *S. erythraea* strain and induce early autolysis of mycelium (Figure 3a). We tested three final concentrations of *E. coli* cells by the co-cultivation system, where the OD_{600} values were 0.02, 0.05, and 0.1, respectively. Under each condition, we encapsulated the spores of *S. erythraea* NRRL 23338 and S3-3, together with Top10/MphR in droplets, respectively, and observed the green fluorescence signals of these droplets at different time intervals by fluorescence microscopy. We found that the droplets containing *S. erythraea* NRRL 23338 did not exhibit obvious green fluorescence even after 7 days of cultivation, while the S3-3-containing droplets showed detectable fluorescence after 1-day cultivation when the final OD_{600} of *E. coli* concentration was 0.02, and after 3-day cultivation when the final OD_{600} of *E. coli* was 0.05 or 0.1 (Figure 3b). Under the condition of *E. coli* OD_{600} = 0.02, erythromycin was produced earlier, and the fluorescence of mycelium-containing droplets is continuously increasing within 3 days, suggesting that this was the best initial ratio of *E. coli* cells in the co-cultivation system. The results were also consistent with the previous fermentation results in a 24-well plate, indicating that S3-3 could similarly produce erythromycin in LB medium in droplets within 3 days. When the time was prolonged to day 5, the background signal of the droplets only containing *E. coli* became stronger due to the accumulation and permeation of erythromycin from *S. erythraea*-containing droplets (Figure 3b). Taking all factors into consideration, we chose day 3 as the sorting time point in the following experiments.

One of the key points for developing a successful co-cultivation-based screening method is to effectively eliminate biosensor strains before downstream fermentation and analysis. Thus, the *S. erythraea*−*E. coli* co-encapsulated droplets were applied on different agar plates, including modified agar medium, R2YE agar medium, and LB agar medium. At the same time, different nalidixic acid concentrations of 10, 20, and 30 μg/mL were added to the medium to test their effectiveness in the growth inhibition of *E. coli*. We found that *S. erythraea* was not sensitive to nalidixic acid, although it grew more slowly when

https://doi.org/10.1021/acssynbio.2c00102
ACS Synth. Biol. 2022, 11, 2697−2708

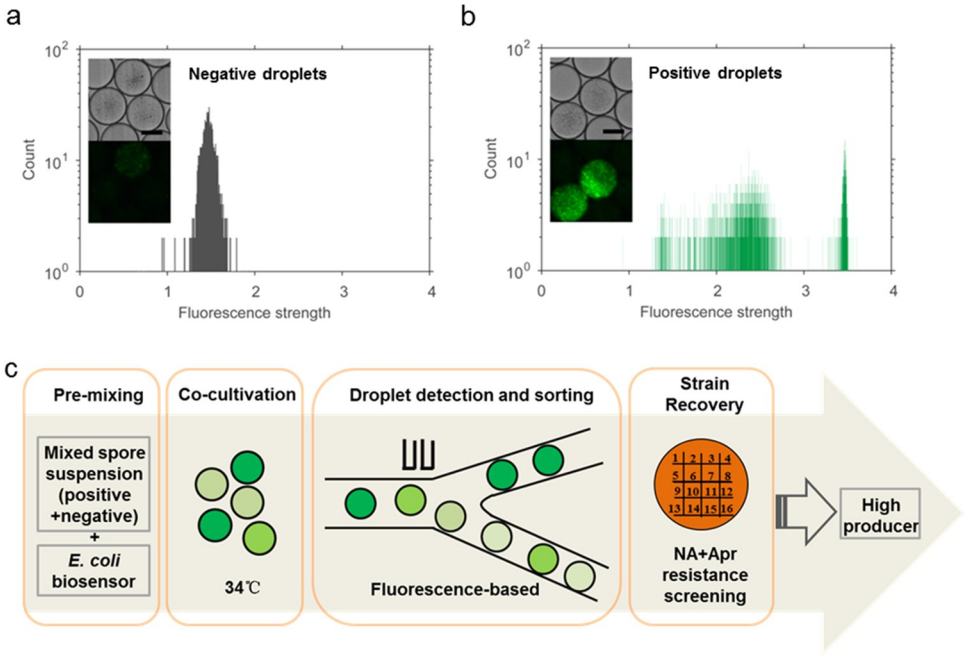

Figure 4. Proof-of-concept screening of an artificial library of different erythromycin productions using WELCOME. (a) Fluorescence signal histogram of negative droplets containing low-producing strain *S. erythraea* NRRL 23338 by FADS analysis. (b) Fluorescence signal histogram of positive droplets containing high-producing strain S3-3 by FADS analysis. Scale bar: 50 μm. (c) Flowchart of WELCOME.

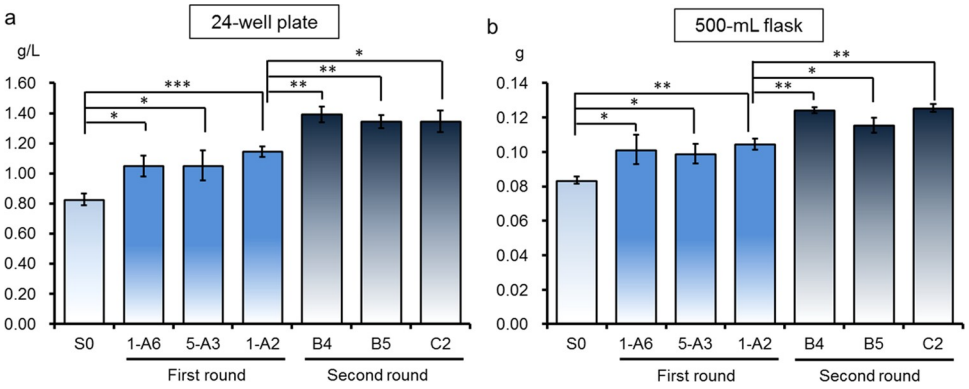

Figure 5. Fermentation results of the high-producing mutants screened in two rounds of WELCOME. The titers in 24-well-plate fermentation (a) and the total yields in 500 mL flask fermentation (b) of the starting strain S0, mutants 1-A6, 5-A3, and 1-A2 obtained in the first-round screening, and mutants B4, B5, and C2 obtained in the second-round screening. Error bars represent the standard deviation of the mean from three biological replicates. $*p \leq 0.05$, $**p \leq 0.01$ and $***p \leq 0.001$ (Student's two-tailed *t*-test).

high-concentration nalidixic acid was added. *E. coli* growth could be totally inhibited by 10 μg/mL nalidixic acid on both modified agar medium and LB agar medium, while *E. coli* thrived on R2YE agar medium even when 30 μg/mL nalidixic acid was present (Figure S4). Considering that *S. erythraea* grew better on the modified agar medium than on the LB agar medium, we chose a modified agar medium containing 10 μg/mL of nalidixic acid to isolate *S. erythraea* from the co-cultivation droplets after sorting.

2.3. Proof-of-Concept Screening of an Artificial Mixture of Strains with Different Erythromycin Productions. To establish the workflow of WELCOME, we intended to conduct a proof-of-concept screening of an artificial mixture of *S. erythraea* NRRL 23338 and S3-3 as the negative and positive strains, respectively, which were proved to have different erythromycin production levels in the previous experiment. The spores of *S. erythraea* NRRL 23338 and S3-3 were co-encapsulated in droplets with Top10/MphR, respectively, and the droplets were first analyzed by FADS after 3-day cultivation. The result showed that the two different droplets exhibited significantly different fluorescence strengths in FADS analysis (Figure 4a,b), which were consistent with the observation by a fluorescence microscope (Figure 3b).

Then, the artificial mixture was constructed by mixing 5% positive S3-3-containing droplets and 95% negative *S. erythraea* NRRL 23338-containing droplets. During sorting, the top 1% of droplets of high green fluorescence signal in the artificial mixture was forced to deflect in 700 V of voltage by FADS. The sorted droplets were applied on nalidixic acid-containing agar plates for *E. coli* elimination. *S. erythraea* S3-3 was apramycin-resistant and can be easily distinguished from the apramycin-sensitive *S. erythraea* NRRL 23338. Therefore, the emerging colonies on agar plates were isolated and passaged both on the nalidixic acid plus apramycin-containing agar plate and on the nalidixic acid-containing agar plate as a control to determine their apramycin resistance (Figure 4c). We found that 94.24% of the isolated colonies were S3-3 that survived under apramycin screening

https://doi.org/10.1021/acssynbio.2c00102
ACS Synth. Biol. 2022, 11, 2697−2708

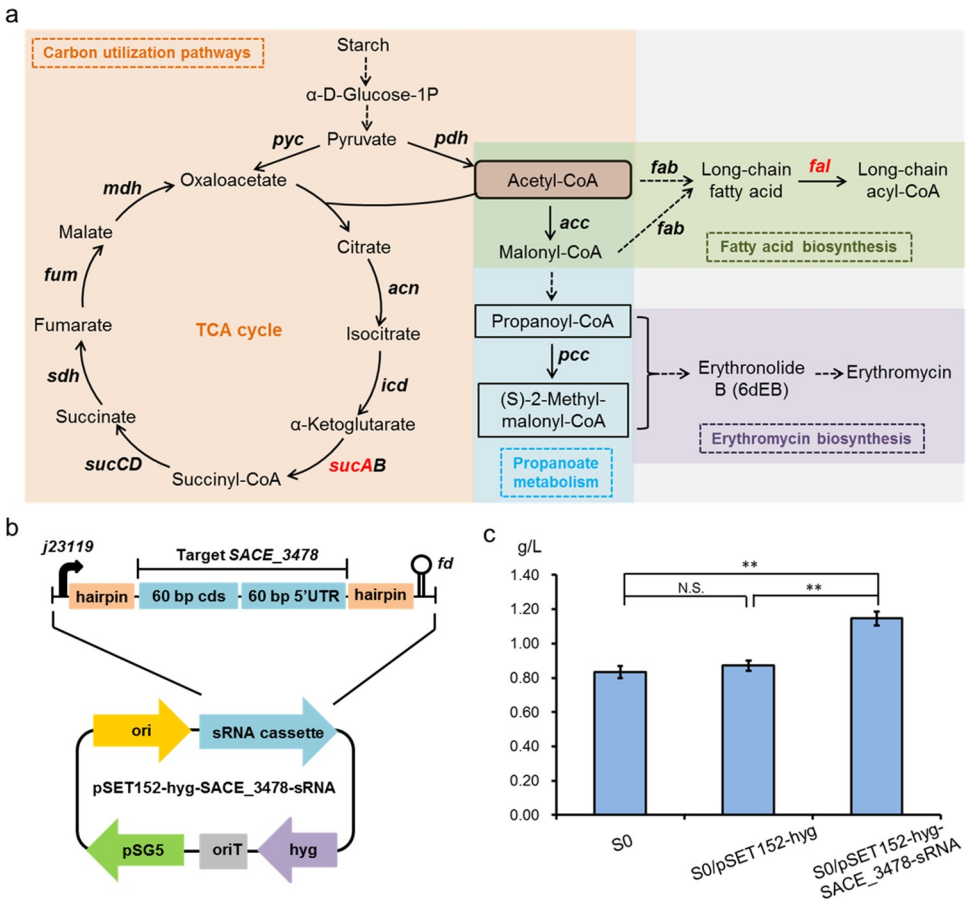

Figure 6. Analysis and verification of the mutated genes in the high-producing mutants. (a) Overview of the important mutated genes of high-producing strains in metabolic pathways and their potential influence on erythromycin biosynthesis. *pyc*, pyruvate carboxylase gene; *pdh*, pyruvate dehydrogenase gene; *acn*, aconitase gene; *icd*, isocitrate dehydrogenase gene; *sucAB*, 2-oxoglutarate dehydrogenase complex gene; *sucCD*, succinyl-CoA synthase gene; *sdh*, succinate dehydrogenase gene; *fum*, fumarase gene; *mdh*, malate dehydrogenase gene; *acc*, acyl-CoA carboxylase complex gene; *pcc*, methylmalonyl-CoA carboxyltransferase gene; *fab*, fatty acid biosynthesis multienzyme system; *fal*, long-chain fatty acid-CoA ligase. Mutated genes are shown in red. Solid arrows indicate one-step reactions, and dotted arrows indicate multistep reactions. (b) Schematic diagram of the pSET152-hyg-SACE_3478-sRNA plasmid for downregulating *SACE_3478* expression. The sRNA expression cassette was composed of j23119 promoter, two 21-bp hairpins that reverse complementary to each other (CAGTGGTGGTGGTGGTGGTGC and GCACCACCACCACCACCACTG), 60-bp reverse complemented sequences in *SACE_3478* coding region, 60-bp reverse complemented sequences in 5′ untranslated region, and fd terminator. (c) Titers in 24-well plate fermentation of strains S0, S0/pSET152-hyg, and S0/pSET152-hyg-SACE_3478-sRNA. Error bars represent the standard deviation of the mean from three biological replicates. $^{**}p \leq 0.01$, and NS indicates no significant difference (Student's two-tailed *t*-test).

(Table S2), indicating an enrichment ratio[15] of 310.9 (Table S3). This result demonstrated that, using WELCOME, *S. erythraea* strain with high erythromycin production can be effectively and efficiently screened out in a mixed library by FADS.

2.4. Iterative Rounds of Mutagenesis and HTS for Strains with Enhanced Erythromycin Production. To demonstrate the application prospects of WELCOME, we intended to screen erythromycin hyperproducers from a random ARTP mutagenesis library of an industrial strain S0, which was already a very high erythromycin producer. Specifically, 7-day-old *S. erythraea* spores were first collected and subjected to ARTP mutagenesis and then regenerated on the modified agar plate for sporulation to generate a random library of *S. erythraea*. The mutant library of around 66,000 variants was co-encapsulated with the biosensor strain Top10/mphR in droplets for 3-day cultivation and then subjected to FADS analysis. The top 1% of droplets with the strongest signals were sorted and collected for further strain isolation and analysis, among which the three most promising mutants, 1-A6, 5-A3, and 1-A2, showed the best fermentation performance. The fermentation results showed that the titers in 24-well plates of 1-A6, 5-A3, and 1-A2 were 1.050 ± 0.069, 1.053 ± 0.101, and 1.145 ± 0.034 g/L, representing 26.8 ± 8.3, 27.2 ± 12.2, and 38.3 ± 4.1% of enhancements, respectively, compared to the starting strain S0 whose titer was 0.828 ± 0.038 g/L under the same fermentation condition (Figure 5a). The total yields in 500 mL flask fermentation of these three mutants were further analyzed and determined to be 0.101 ± 0.008, 0.099 ± 0.006, and 0.105 ± 0.003 g, exhibiting 20.2 ± 9.5, 17.9 ± 7.1, and 25.0 ± 3.6% of improvements compared to the S0 strain whose yield was 0.084 ± 0.002 g, respectively (Figure 5b). This result demonstrated that, with the help of WELCOME, strains with enhanced erythromycin productions can be successfully and rapidly identified from a large random mutation library in one-round HTS by FADS.

Iterative mutagenesis and HTS were efficient strategies to breed better microorganisms.[16−18] To further improve erythromycin production, we started from mutant 1-A2, which was the best mutant in the first-round screening, and conducted the

https://doi.org/10.1021/acssynbio.2c00102
ACS Synth. Biol. 2022, 11, 2697−2708

second round of ARTP mutagenesis and FADS screening in a similar way. After the second-round WELCOME, three best mutants, B4, B5, and C2, were determined to produce 1.391 ± 0.050, 1.344 ± 0.044, and 1.345 ± 0.073 g/L of erythromycin in 24-well plate fermentation, exhibiting 21.5 ± 4.4, 17.4 ± 3.8, and 17.5 ± 6.4% improved titer compared to the starting strain 1-A2, respectively (Figure 5a). In 500 mL flask fermentation, the total yields of these three mutants were 0.124 ± 0.002, 0.116 ± 0.004, and 0.126 ± 0.002 g, respectively, representing 18.1 ± 1.9, 10.5 ± 3.8, and 20.0 ± 1.9% improvements compared to that of the 1-A2 strain (Figure 5b). Notably, compared to the initial starting strain S0, we successfully obtained the best mutant C2 from iterative mutagenesis and HTS exhibiting 62.4% titer and 50.0% yield improvement in 24-well plate and 500 mL flask fermentation, respectively. Despite the enhanced productions, erythromycin compositions of the fermentation broths of six screened mutants were similar to that of the starting strain by LC-MS analysis (Figure S5).

2.5. Genome Sequencing and Analysis of the Mutants Obtained by WELCOME. To analyze the potential mechanisms for high production in mutant strains, the six mutants obtained in two rounds of screening, 1-A6, 5-A3, 1-A2, B4, B5, and C2, were subjected to genome sequencing and analysis. Compared to the starting strain S0, totally 16 mutations, including 2 insertions, 4 deletions, and 10 single nucleotide variations, were identified among the three first-round mutants 1-A6, 5-A3, and 1-A2, in which 12 mutations were located in the coding regions (Table S4). In terms of the three second-round mutants, B4, B5, and C2, the newly generated mutations compared to the starting strain 1-A2 were also 16, displaying 2 insertions, 2 deletions, and 12 single nucleotide variations, 10 of which were located in the coding regions (Table S5). Interestingly, all six mutants shared a 4 bp deletion in gene *SACE*_3478 coding long-chain fatty acid-CoA ligase (AMP-dependent synthetase/ligase) involved in the fatty acid biosynthesis, which would induce a frame-shift mutation and a consequent loss of function of its coding product. *S. erythraea* was closely related to *Streptomyces* species that only possess type II fatty acid biosynthesis (FAS II) pathway, in which a multienzyme system is responsible for converting extender units acetyl-CoA and malonyl-CoA to long-chain fatty acid after a series of reactions[19] (Figure 6a). Then, long-chain fatty acid-CoA ligase would catalyze the long-chain fatty acid to the final product long-chain fatty acid-CoA in fatty acid biosynthesis, which will be used to synthesize complex lipids. On the other hand, acetyl-CoA and malonyl-CoA were also the key precursors that can be transformed into propionyl-CoA and (*S*)-2-methyl-malonyl-CoA through propanoate metabolism, which would be used as extender units in the erythromycin biosynthesis.[20] Thus, the inactivation of long-chain fatty acid-CoA ligase may reduce the competition for acetyl-CoA and malonyl-CoA by hindering fatty acid biosynthesis and consequently enhanced metabolic flux through erythromycin biosynthesis and production (Figure 6a).

We also recognized another two metabolism-associated SNPs located in gene *SACE*_6385 that were shared by three mutants B4, B5, and C2. *SACE*_6385 (*sucA*) encodes 2-oxoglutarate dehydrogenase E1 module, which catalyzes a rate-limiting step of the tricarboxylic acid cycle (TCA) of aerobe.[21] Two amino acid substitutions, F320L and Y571H, were induced by the mutations of *sucA*, and one substitution Y571H was located in the TPP (Thiamine pyrophosphate)-binding domain, which may influence enzyme activity.[22] Coincidentally, in a previously reported work, *sucA* and *sucB*, coding two components of 2-oxoglutarate dehydrogenase, in another high erythromycin production strain *S. erythraea* Px were also found to be mutated compared to the wild-type *S. erythraea* NRRL 23338.[23] Since 2-oxoglutarate dehydrogenase was commonly conserved in bacteria, one possible explanation for this coincidence is that the activity alteration of 2-oxoglutarate dehydrogenase will influence the metabolic flux through the TCA cycle and consequently enhanced the supply of acetyl-CoA, which is the key node of primary and secondary metabolic pathways, to the alternative propanoate metabolism. This potential redistribution of primary metabolites may help synthesize more extender units and thus enhance erythromycin biosynthesis (Figure 6a).

We also noted that four mutants obtained in different rounds of screening, 1-A6, 5-A3, B4, and B5, shared a 17.2 kb deletion that encoded one integrase and several hypothetical proteins. This region was deduced to be the phage-derived integrative plasmid pSE211, which was harbored by both the wild-type strain *S. erythraea* NRRL 23338 and the parental strain *S. erythraea* S0.[24] Similarly, 11 kb deletion of a prophage was also reported in another high-erythromycin-production *S. erythraea* strain E3 compared to *S. erythraea* NRRL 23338.[25] Although the mechanism of enhanced erythromycin production induced by prophage deletion was unclear, we speculated that the reduced genome may bring better genome stability and release some metabolic burden of mutants.

2.6. Metabolic Engineering of *S. erythraea* to Confirm the Function of *SACE*_3478 in Erythromycin Production. In previous attempts, we failed to transform the *pSG5*-derived replicative plasmid into S0, which rendered knockout *SACE*_3478 in this strain impossible at present. Hence, to investigate the role of gene *SACE*_3478 in erythromycin production, we decided to use an integrative plasmid and antisense RNA (sRNA) interference strategy to downregulate gene expression.[26] pSET152-derived plasmid harboring sRNA expression cassette targeting *SACE*_3478 was integrated into S0 genome to construct strain S0/pSET152-hyg-SACE_3478-sRNA, where *SACE*_3478 expression was hindered by the 120 bp of reverse complementary sRNA sequences targeting the mRNA of *SACE*_3478 (Figure 6b). Strain S0/pSET152-hyg carrying a blank plasmid was used as the control. The fermentation result showed that downregulation of *SACE*_3478 expression induced 31.6% increased erythromycin titer compared to S0/pSET152-hyg, which confirmed our hypothesis that inactivation of *SACE*_3478 in our screened mutants improved erythromycin production, and fatty acid biosynthesis is a promising target pathway for higher production in further strain engineering (Figure 6c).

3. DISCUSSION

Many actinomycetes species are heavily employed in industrial fermentation to produce value-added secondary metabolites. However, industrial actinomycete strains are often intractable in genetic manipulation, which hinders rational strain engineering, leading to the heavy reliance on random mutagenesis methods with generally low positive mutation rates. Moreover, the throughput in the screening process is often limited by the low-efficient plate/flask-based cultivation and screening methods, making strain breeding a labor-intensive and time-consuming process in the industry. To conquer this problem, we developed the droplet-based microfluidic platform to facilitate HTS of actinomycetes, which supports a high throughput of at least 10,000 variants per hour that is thousands of times higher than

https://doi.org/10.1021/acssynbio.2c00102
ACS Synth. Biol. 2022, 11, 2697−2708

the traditional screening processes.[6] Previously, we have demonstrated the extensive applications of the droplet-based microfluidic platform on the HTS of regulatory elements in the early stage and proteins in the middle stage. In this study, combining the whole-cell biosensor with the microfluidic platform, we established WELCOME to further extend its application potential in the product-driven screening of actinomycete secondary metabolites, which are usually produced in the late stage of fermentation. The versatile applications of the droplet-based microfluidic platform are guaranteed by the long-term stability of actinomycete-containing droplets. This platform can assist the HTS of the generated large-scale libraries of actinomycetes in random mutagenesis and accelerate the process of strain engineering in the industry.

When conducting product-driven screening, biosensors are good intermediaries between "invisible" productions and "visualized" outputs. The HTS based on biosensor-producer co-cultivation relies on the whole-cell biosensor in the genetic-tractable host and bypasses any requirement of genetic modification of producing strain, which is impossible for most industrial strains. Starting from an industrial strain of high erythromycin production, we successfully screened out six mutants with hyperproductions from two rounds of WELCOME within 3 months, one of which exhibits 50% improvement on total yield compared to the starting strain. Besides, the genomic analysis of those mutant strains also provides insights into the mechanisms of high antibiotic production. In two rounds of screening, we summarized that *SACE*_3478 coding a long-fatty acid-CoA ligase was inactivated in all of the six screened mutants, and *sucA* coding 2-oxoglutarate dehydrogenase E1 component was mutated in three mutants. By means of downregulating gene expression, we confirmed that *SACE*_3478 had a negative effect on erythromycin biosynthesis, and the fatty acid biosynthesis pathway will be a potential target pathway for rational strain engineering. We speculate that the reduced metabolic flux through fatty acid biosynthesis and TCA cycle will make acetyl-CoA funneled into the alternative propanoate metabolism, and consequently enhance erythromycin biosynthesis. Also, a 17.2 kb integrative plasmid pSE211 inherited from the wild-type strain was found to be deleted in four high-producing mutants, indicating that prophage deletion might be a possible strategy to increase production in some cases. The mutated genes that are shared by several screened strains of hyperproductions may be promising targets for further metabolic engineering. In this work, we used an MphR-based biosensor to facilitate erythromycin screening. Indeed, MphR protein is a powerful tool for the HTS of various macrolides, not only due to its ligand promiscuity but also because its specificity to effector molecules could be altered via protein engineering.[13] For instance, the in vivo production of clarithromycin, a semisynthetic analogue of erythromycin, can be recognized by an improved MphR variant through multistrategy protein engineering.[27] Besides MphR, the TetR family also contributes to the most abundant members of transcription factors in actinobacteria, many of which are proved to be strongly related to secondary biosynthesis.[28,29] The metabolite-specific biosensors constructed based on the regulatory elements in the secondary biosynthetic clusters are also promising tools in the HTS of interesting products.[30]

Previous works have provided some examples that demonstrated the feasibility of the biosensor-producer co-cultivation strategy in the screening of small molecules.[31−33] Nevertheless, it is worth noting that there are some limitations of this strategy in applications. The most pivotal issue is the unavoidable competition of biosensors and producers in droplets. *E. coli* strains were usually employed as the biosensor hosts in most co-cultivation systems, which is due to their easy genetic manipulation. However, compared to the fast-growing *E. coli* cells, other model strains with relatively low growth rates, such as *Corynebacterium glutamicum*, *Bacillus subtilis,* and yeast, may reduce the competition of nutrition and living space with producers in a limited system, and thus may be better alternative biosensor hosts in some co-cultivation applications. On the other hand, in the era of synthetic biology, fine-tuning of growth of *E. coli* to be more compatible with WELCOME is also feasible. In addition, better selectivity of co-cultivation-based HTS can be achieved by introducing some growth-linked features such as constructing an auxotrophic biosensor strain, which will survive or grow better in the presence of the target product.[34,35] Moreover, researches flourish in recent years on cell-free protein synthesis systems for the detection of small molecules.[36] These in vitro biosensors, usually demonstrating more robustness, may circumvent the competition of biosensors and producing strains in the co-cultivation mode, and provide more options in certain applications.[37,38]

4. MATERIALS AND METHODS

4.1. Strains, Media, and Cultivation Conditions. The strains used in this study are listed in Table S6. Strains *S. erythraea* NRRL 23338 and S0 were the low-producing and high-producing erythromycin producers, respectively. Strain *S. erythraea* S3-3 derived from S0 integrated with pSET152 was the apramycin-resistant strain of high erythromycin production. Modified agar medium was used for spore germination of *S. erythraea*, whose composition was as follows: starch, 10 g/L; corn syrup, 12 g/L; NaCl, 3 g/L; $CaCO_3$, 3 g/L; agar powder, 20 g/L (pH = 6.8−7.0). R2YE agar medium[39] and LB agar medium were also used for the verification of the growth of *S. erythraea*, and *E. coli*. LB liquid medium was used for *E. coli* cultivation, erythromycin production in 24- and 96-well plates and spore germination in droplets. Agar plates and droplets were incubated at 34 °C. The 24-well plates were shaken at 34 °C and 250 rpm, while 96-well plates were shaken at 34 °C and 800 rpm. When necessary, 50 μg/mL ampicillin and 50 μg/mL chloramphenicol were supplied for the cultivation of *E. coli* biosensor strains, 50 μg/mL apramycin and 80 μg/mL hygromycin were added for the cultivation of apramycin- or hygromycin-resistant *S. erythraea* strains, respectively, and 10 μg/mL nalidixic acid was used to inhibit *E. coli* growth in strain isolation.

4.2. Construction of *E. coli* Biosensor Strains. The plasmids constructed in this study are listed in Table S6. The expression cassettes P_{lac}-*mphr*, P_{lac}-*m2d6*, and *mpha* were synthesized to pUC57 plasmid according to the literature,[13] respectively, generating pUC57-P_{lac}-mphr, pUC57-P_{lac}-m2d6, and pUC57-mpha. Then, P_{mphR}-*gfp* expression cassette was amplified and assembled with pUC57-P_{lac}-mphr and pUC57-P_{lac}-m2d6 by in vitro homologous recombination, respectively, generating two biosensor plasmids, pMphR and pM2D6. *mpha* was amplified and ligated to pACYC backbone to construct pMphA plasmid. Then, pMphR or pM2D6 was co-transformed together with pMphA to the recipient cell *E. coli* Top10 to generate *E. coli* biosensor strain Top10/pMphA&pMphR (abbreviated to Top10/MphR) or Top10/pMphA&pM2D6 (abbreviated to Top10/M2D6). Primers used in this study are listed in Table S7.

https://doi.org/10.1021/acssynbio.2c00102
ACS Synth. Biol. 2022, 11, 2697−2708

4.3. Dose−Response Detection of *E. coli* Biosensor Strain. Erythromycin stock solution (10 mM) was diluted with sterilized water to a series of concentrations of 1, 2.5, 7.5, 10, 20, 50, 100, 200, 500, 1000, and 2000 μM. Overnight-cultured *E. coli* biosensor broths were transferred by 2% into LB medium and cultivated at 37 °C and 220 rpm until the OD_{600} was 0.6. The cells were collected by centrifugation, washed three times with LB medium, and suspended in LB medium to a final OD_{600} of 0.6. For each well of the 96-well plate, 810 μL of strain culture and 90 μL of diluted erythromycin solution were added and mixed, where the erythromycin was 10-fold diluted in the final mixture. Thus, the working concentrations of erythromycin were 0.1, 0.25, 0.75, 1, 2, 5, 10, 20, 50, 100, and 200 μM. Strain culture (810 μL) mixed with 90 μL of sterilized water was used as the blank control. For each condition, three replicates were set to ensure accuracy. The strain-containing 96-well plates were shaken at 34 °C, 800 rpm, or statically cultivated at 34 °C in the incubator. Fluorescence analysis was conducted at different time intervals of 1, 2, 3, 5, and 7 days. At each time point, for each well, 100 μL of strain culture was absorbed and transferred to a 96-well ELISA plate for fluorescence detection (Ex 488 nm/Em 520 nm) using a microplate reader (Bio Tek, Neo2). The fluorescence intensity was divided by the corresponding cell density value (OD_{600}) to calculate the normalized GFP fluorescence value of each sample.

4.4. Droplet Generation and Microfluidic Screening. The microfluidic droplet-making device and sorting device[6] were kindly provided by Harvard University. Droplets were generated as follows: For the preparation of *S. erythraea* spore suspension, 7-day-old *S. erythraea* spores were collected and suspended in 3 mL of LB liquid medium and filtered through eight-layered sterilized lens paper to remove mycelium. Then, the filtrate was added into a 1.5 mL 10 kDa cutoff protein concentrator (Millipore), washed three times with 400 μL of LB medium to remove erythromycin, and resuspended in 400 μL of LB medium. The spore suspension was diluted to a final concentration of 1×10^6 spores/mL. For the preparation of *E. coli* suspension, overnight-cultured biosensor *E. coli* strain broth was used as the seed culture and transferred into LB medium to a resultant OD_{600} of 0.1. The strain culture was cultivated at 37 °C and 220 rpm until the OD_{600} became 0.6. Then, the *E. coli* cells were centrifuged for collection, washed twice with LB medium to remove antibiotics, and resuspended in antibiotic-free LB medium to a final OD_{600} of 0.1. The mixture of 1 mL of *S. erythraea* spore suspension (1×10^6 spores/mL) and 250 μL of *E. coli* suspension was used as the aqueous phase, which was pumped at a flow rate of 400 μL/h. HFE-7500 fluorinated fluid (3 M) with 1.0% (w/w) surfactant (RAN Biotechnologies) was used as the carrier oil phase and pumped at a flow rate of 800 μL/h. The resultant diameter of droplets was around 90 nm. The generated droplets were collected in a 1 mL syringe or a 1.5 mL tube and incubated at 34 °C for 3 days for further analysis.

When sorting, the droplets were pumped into the sorting device at a flow rate of 20 μL/h. HFE-7500 was used as the spacing oil and pumped at a flow rate of 1000 μL/h to separate droplets. The droplets were focused with a 20× objective and excited by a 488 nm laser. The emitted 520 nm fluorescence signal was detected by the photomultiplier tube (PMT). Target droplets with desired fluorescence intensities were forced by 700 V of voltage to deflect into the sorting channel in the electric field and collected in a 1.5 mL tube, while the unwanted droplets were rejected through the waste channel. The average sorting frequency was 15 Hz. The collected droplets were spread on a modified agar plate (supplemented with 10 μg/mL nalidixic acid) and cultivated at 34 °C for 7 days, and the emerging colonies were picked for further cultivation and analysis.

4.5. Fluorescence Microscopy of *S. erythraea*−*E. coli* Co-Cultivation Droplets. Co-encapsulated droplets (3 μL) surrounded with 15−20 μL of oil phase were added to a hemocytometer and observed using a fluorescence microscope (Leica DM5000B) under a 20× objective lens (Ex 488 nm/Em 520 nm). When taking fluorescent pictures, the exposure time was 50 ms.

4.6. ARTP Mutagenesis. ARTP mutagenesis was performed to generate a random library of *S. erythraea*. Seven-day-old *S. erythraea* spores were collected from a modified agar plate and suspended in sterilized water. Then, the spore suspension was washed twice with sterilized water to remove erythromycin and filtered through eight-layered sterilized lens paper to remove mycelium. The filtrate was diluted with sterilized water to a final concentration of 1×10^8 spores/mL. Then, 100 μL of the spore suspension was spread onto 10 sterilized steel dishes (10 μL per dish). The dishes were exposed to a helium gas flow for 90 s and washed vigorously with 1 mL of LB medium. The spore suspension was incubated at 34 °C for 3 h and then spread on the modified agar plates and cultivated at 34 °C for 7 days for sporulation. The spores were collected and treated in a similar way as described in the droplet generation part to remove mycelium and erythromycin contamination. The spore concentration in the filtrate was determined by microscopy. Then, the filtrate was diluted by LB liquid medium to a final concentration of 1×10^6 spores/mL. The spore suspension (640 μL) was mixed with 160 μL of 0.1 OD *E. coli* biosensor cell suspension, and the mixture was used as the aqueous phase to generate droplets.

4.7. Strain Fermentation and Evaluation of Erythromycin Production. Fermentation of the high-producing mutants obtained from screening was performed in 24-well plates containing 3 mL of medium under 32 °C and 250 rpm or in 500 mL flasks containing 50 mL of medium under 32 °C and 220 rpm. In 24-well-plate fermentation, the seed medium was prepared as follows: glucose, 10 g/L; tryptone, 4 g/L; yeast extract, 4 g/L; $MgSO_4$, 0.5 g/L; KH_2PO_4, 2.0 g/L; K_2HPO_4, 4 g/L, and the fermentation medium was prepared as follows: starch, 20 g/L; dextrin, 20 g/L; soybean powder, 15 g/L; $(NH_4)_2SO_4$, 4 g/L; $CaCO_3$, 6 g/L; soybean oil, 5 mL/L. After 3-day cultivation, 300 μL of seed broth was transferred into 3 mL of fermentation medium for another 7-day cultivation. In 500 mL flask fermentation, the seed medium was prepared as follows: starch, 25 g/L; dextrin, 25 g/L; corn syrup, 13 g/L; soybean powder, 18 g/L; NaCl, 3 g/L; $(NH_4)_2SO_4$, 1.2 g/L; NH_4NO_3, 1.2 g/L; $CaCO_3$, 6 g/L; soybean oil, 4 mL/L, and the fermentation medium was prepared as follows: starch, 70 g/L; soybean powder, 30 g/L; $(NH_4)_2SO_4$, 2 g/L; $CaCO_3$, 6 g/L; soybean oil, 9 mL/L; *n*-propanol, 10 mL/L (added after 1-day cultivation). Similarly, 5 mL of 3-day-old seed broth was transferred into 50 mL of fermentation medium subjected to further 7-day cultivation.

A modified colorimetric method was used to evaluate the erythromycin titer of each sample in a 24-well plate and 500 mL flask fermentation.[40,41] The total yield in 500 mL flask fermentation was calculated by multiplying the titer and the corresponding broth volume at the end of fermentation. Erythromycin composition of each sample was determined by positive-ion-mode LC-MS analysis using C_{18} column at 30 °C. The mobile phases were composed of solvent A (0.1% formic

https://doi.org/10.1021/acssynbio.2c00102
ACS Synth. Biol. 2022, 11, 2697−2708

acid solution) and solvent B (acetonitrile), and the linear gradient program was as follows: 10−95% solvent B in 0−30 min, 95% solvent B in 31−39 min, and 10% solvent B in 40−50 min at a flow rate of 0.3 mL/min. UV signals were detected at 215 nm.

4.8. Whole Genome Sequencing and Mutation Analysis. Strains were cultivated in seed medium in a 24-well plate under 34 °C and 250 rpm for 3 days. After cultivation, the genomic DNA of mycelium was extracted according to the manufacturer's protocols (BIOMIGA Bacterial gDNA Isolation Kit, China). Illumina NovaSeq. 6000 sequencing platform was used to construct and sequence the genomic libraries by Novogene (Beijing, China), and the generated reads were mapped to *S. erythraea* NRRL 23338 reference genome with accession number NC_009142 on NCBI website. Breseq software was used to determine the mutations of each strain.

■ ASSOCIATED CONTENT

Supporting Information

The Supporting Information is available free of charge at https://pubs.acs.org/doi/10.1021/acssynbio.2c00102.

Green fluorescence response with and without 10 μM erythromycin of *E. coli* strains Top10, Top10/MphR, and Top10/M2D6 (Figure S1); dose−response curves of *E. coli* biosensor strains Top10/MphR (MphR) and Top10/M2D6 (M2D6) under shaking and static conditions at different time intervals (Figure S2); comparison of different washing methods in removing erythromycin background (Figure S3); optimization of pure cultivation condition of *S. erythraea* strains (Figure S4); erythromycin component analysis of S0 and six mutants by LC-MS detection (Figure S5); comparison of the colony numbers on antibiotic-free LB agar plates and chloramphenicol and ampicillin-containing LB agar plates (Table S1); positive rates of FADS experiments (Table S2); enrichment ratio of FADS (Table S3); mutations compared to the starting strain S0 in the mutants 1-A2, 1-A6, and 5-A3 obtained in the first-round screening (Table S4); newly generated mutations compared to the starting strain 1-A2 in the mutants B4, B5, and C2 obtained in the second-round screening (Table S5); strains and plasmids used in this study (Table S6); and primers used in this study (Table S7) (PDF)

■ AUTHOR INFORMATION

Corresponding Authors

Yue Zhang − *Tianjin Institute of Industrial Biotechnology, Chinese Academy of Sciences, Tianjin 300308, China; Haihe Laboratory of Synthetic Biology, Tianjin 300308, China; Key Laboratory of Systems Microbial Biotechnology, Chinese Academy of Sciences, Tianjin 300308, China;* orcid.org/0000-0002-4383-6313; Email: zhangy@tib.cas.cn

Ran Tu − *Tianjin Institute of Industrial Biotechnology, Chinese Academy of Sciences, Tianjin 300308, China; Key Laboratory of Systems Microbial Biotechnology, Chinese Academy of Sciences, Tianjin 300308, China*; Email: tu_r@tib.cas.cn

Meng Wang − *Tianjin Institute of Industrial Biotechnology, Chinese Academy of Sciences, Tianjin 300308, China; Haihe Laboratory of Synthetic Biology, Tianjin 300308, China; Key Laboratory of Systems Microbial Biotechnology, Chinese Academy of Sciences, Tianjin 300308, China;* orcid.org/0000-0001-7648-9955; Email: wangmeng@tib.cas.cn

Authors

Erbing Hua − *College of Biotechnology, Tianjin University of Science and Technology, Tianjin 300457, China*

Kaiyue Yun − *College of Biotechnology, Tianjin University of Science and Technology, Tianjin 300457, China; Tianjin Institute of Industrial Biotechnology, Chinese Academy of Sciences, Tianjin 300308, China; Key Laboratory of Systems Microbial Biotechnology, Chinese Academy of Sciences, Tianjin 300308, China*

Wenjia Pan − *Tianjin Institute of Industrial Biotechnology, Chinese Academy of Sciences, Tianjin 300308, China; Key Laboratory of Systems Microbial Biotechnology, Chinese Academy of Sciences, Tianjin 300308, China*

Ye Liu − *Tianjin Institute of Industrial Biotechnology, Chinese Academy of Sciences, Tianjin 300308, China; Key Laboratory of Systems Microbial Biotechnology, Chinese Academy of Sciences, Tianjin 300308, China*

Shixin Li − *College of Biotechnology, Tianjin University of Science and Technology, Tianjin 300457, China; Tianjin Institute of Industrial Biotechnology, Chinese Academy of Sciences, Tianjin 300308, China; Key Laboratory of Systems Microbial Biotechnology, Chinese Academy of Sciences, Tianjin 300308, China*

Yan Wang − *College of Biotechnology, Tianjin University of Science and Technology, Tianjin 300457, China; Tianjin Institute of Industrial Biotechnology, Chinese Academy of Sciences, Tianjin 300308, China; Key Laboratory of Systems Microbial Biotechnology, Chinese Academy of Sciences, Tianjin 300308, China*

Complete contact information is available at: https://pubs.acs.org/10.1021/acssynbio.2c00102

Author Contributions

‖E.H. and Y.Z contributed equally to this work. M.W. supervised the project. M.W., R.T., and Y.Z. conceived and designed this project. Y.Z., R.T., K.Y., W.P., Y.L., S.L., and Y.W. performed the experiments. E.H. gave advice to the experiments. Y.Z. and R.T. analyzed the data. Y.Z. wrote the manuscript. M.W., R.T., and Y.Z. revised the manuscript.

Notes

The authors declare no competing financial interest.

■ ACKNOWLEDGMENTS

This work was supported by the National Key R&D Program of China (2019YFA0905700 and 2021YFC2100201), "Key Research Project" of Haihe Laboratory of Synthetic Biology and Tianjin Synthetic Biotechnology Innovation Capacity Improvement Project (TSBICIP-PTJS-003 and TSBICIP-KJGG-006). The authors also thank Dr. Xiaoping Liao for his work on NGS data analysis.

■ REFERENCES

(1) Barka, E. A.; Vatsa, P.; Sanchez, L.; et al. Taxonomy, Physiology, and Natural Products of Actinobacteria. *Microbiol. Mol. Biol. Rev.* **2016**, *80*, 1−43.

(2) Weber, T.; Charusanti, P.; Musiol-Kroll, E. M.; et al. Metabolic engineering of antibiotic factories: new tools for antibiotic production in actinomycetes. *Trends Biotechnol.* **2015**, *33*, 15−26.

(3) Chen, J.; Liu, M.; Liu, X.; et al. Interrogation of *Streptomyces avermitilis* for efficient production of avermectins. *Synth. Syst. Biotechnol.* **2016**, *1*, 7−16.

(4) Gao, Q.; Tan, G. Y.; Xia, X.; Zhang, L. Learn from microbial intelligence for avermectins overproduction. *Curr. Opin. Biotechnol.* **2017**, *48*, 251−257.
(5) Zeng, W.; Guo, L.; Xu, S.; Chen, J.; Zhou, J. High-throughput screening technology in industrial biotechnology. *Trends Biotechnol.* **2020**, *38*, 888−906.
(6) Tu, R.; Zhang, Y.; Hua, E.; et al. Droplet-based microfluidic platform for high-throughput screening of *Streptomyces*. *Commun. Biol.* **2021**, *4*, No. 647.
(7) Schallmey, M.; Frunzke, J.; Eggeling, L.; Marienhagen, J. Looking for the pick of the bunch: high-throughput screening of producing microorganisms with biosensors. *Curr. Opin. Biotechnol.* **2014**, *26*, 148−154.
(8) Binder, S.; Schendzielorz, G.; Stäbler, N.; et al. A high-throughput approach to identify genomic variants of bacterial metabolite producers at the single-cell level. *Genome Biol.* **2012**, *13*, No. R40.
(9) Tang, S. Y.; Cirino, P. C. Design and application of a mevalonate-responsive regulatory protein. *Angew. Chem. Int. Ed.* **2011**, *50*, 1084−1086.
(10) Cheng, F.; Tang, X. L.; Kardashliev, T. Transcription factor-based biosensors in high-throughput screening: advances and applications. *Biotechnol. J.* **2018**, *13*, No. e1700648.
(11) Siedler, S.; Schendzielorz, G.; Binder, S.; et al. SoxR as a single-cell biosensor for NADPH-consuming enzymes in *Escherichia coli*. *ACS Synth. Biol.* **2014**, *3*, 41−47.
(12) Schendzielorz, G.; Dippong, M.; Grünberger, A.; et al. Taking control over control: use of product sensing in single cells to remove flux control at key enzymes in biosynthesis pathways. *ACS Synth. Biol.* **2014**, *3*, 21−29.
(13) Kasey, C. M.; Zerrad, M.; Li, Y.; Cropp, T. A.; Williams, G. J. Development of transcription factor-based designer macrolide biosensors for metabolic engineering and synthetic biology. *ACS Synth. Biol.* **2018**, *7*, 227−239.
(14) Zheng, J.; Sagar, V.; Smolinsky, A.; et al. Structure and function of the macrolide biosensor protein, MphR(A), with and without erythromycin. *J. Mol. Biol.* **2009**, *387*, 1250−1260.
(15) Baret, J. C.; Miller, O. J.; Taly, V.; et al. Fluorescence-activated droplet sorting (FADS): efficient microfluidic cell sorting based on enzymatic activity. *Lab Chip* **2009**, *9*, 1850−1858.
(16) Jiang, Y.; Shang, Y. P.; Li, H.; et al. Enhancing transglutaminase production of *Streptomyces mobaraensis* by iterative mutagenesis breeding with atmospheric and room-temperature plasma (ARTP). *Bioresour. Bioprocess* **2017**, *4*, No. 37.
(17) Zhou, G.; Tian, X.; Lin, Y.; Zhang, S.; Chu, J. Rational high-throughput system for screening of high sophorolipids-producing strains of *Candida bombicola*. *Bioprocess Biosyst. Eng.* **2019**, *42*, 575−582.
(18) Shin, C. H.; Cho, H. S.; Won, H. J.; et al. Enhanced production of clavulanic acid by improving glycerol utilization using reporter-guided mutagenesis of an industrial *Streptomyces clavuligerus* strain. *J. Ind. Microbiol. Biotechnol.* **2021**, *48*, No. kuab004.
(19) Gago, G.; Diacovich, L.; Arabolaza, A.; Tsai, S. C.; Gramajo, H. Fatty acid biosynthesis in actinomycetes. *FEMS Microbiol. Rev.* **2011**, *35*, 475−497.
(20) Wang, Y.; Pfeifer, B. A. 6-Deoxyerythronolide B production through chromosomal localization of the deoxyerythronolide B synthase genes in *E. coli*. *Metab. Eng.* **2008**, *10*, 33−38.
(21) Frank, R. A.; Price, A. J.; Northrop, F. D.; Perham, R. N.; Luisi, B. F. Crystal structure of the E1 component of the *Escherichia coli* 2-oxoglutarate dehydrogenase multienzyme complex. *J. Mol. Biol.* **2007**, *368*, 639−651.
(22) Lu, S.; Wang, J.; Chitsaz, F.; et al. CDD/SPARCLE: the conserved domain database in 2020. *Nucleic Acids Res.* **2020**, *48*, D265−D268.
(23) Peano, C.; Talà, A.; Corti, G.; et al. Comparative genomics and transcriptional profiles of *Saccharopolyspora erythraea* NRRL 2338 and a classically improved erythromycin over-producing strain. *Microb. Cell Fact.* **2012**, *11*, No. 32.
(24) Oliynyk, M.; Samborskyy, M.; Lester, J. B.; et al. Complete genome sequence of the erythromycin-producing bacterium *Saccharopolyspora erythraea* NRRL23338. *Nat. Biotechnol.* **2007**, *25*, 447−453.
(25) Li, Y. Y.; Chang, X.; Yu, W. B.; et al. Systems perspectives on erythromycin biosynthesis by comparative genomic and transcriptomic analyses of *S. erythraea* E3 and NRRL23338 strains. *BMC Genomics* **2013**, *14*, No. 523.
(26) Zhang, Y.; Yun, K.; Huang, H.; et al. Antisense RNA Interference-Enhanced CRISPR/Cas9 Base Editing Method for Improving Base Editing Efficiency in *Streptomyces lividans* 66. *ACS Synth. Biol.* **2021**, *10*, 1053−1063.
(27) Li, Y.; Reed, M.; Wright, H. T.; Cropp, T. A.; Williams, G. J. Development of genetically encoded biosensors for reporting the methyltransferase-dependent biosynthesis of semisynthetic macrolide antibiotics. *ACS Synth. Biol.* **2021**, *10*, 2520−2531.
(28) Romero-Rodríguez, A.; Robledo-Casados, I.; Sanchez, S. An overview on transcriptional regulators in *Streptomyces*. *Biochim. Biophys. Acta, Gene Regul. Mech.* **2015**, *1849*, 1017−1039.
(29) Cuthbertson, L.; Nodwell, J. R. The TetR family of regulators. *Microbiol. Mol. Biol. Rev.* **2013**, *77*, 440−475.
(30) Rebets, Y.; Schmelz, S.; Gromyko, O.; et al. Design, development and application of whole-cell based antibiotic-specific biosensor. *Metab. Eng.* **2018**, *47*, 263−270.
(31) Siedler, S.; Khatri, N. K.; Zsohár, A.; et al. Development of a bacterial biosensor for rapid screening of yeast *p*-coumaric acid production. *ACS Synth. Biol.* **2017**, *6*, 1860−1869.
(32) Meyer, A.; Pellaux, R.; Potot, S.; et al. Optimization of a whole-cell biocatalyst by employing genetically encoded product sensors inside nanolitre reactors. *Nat. Chem.* **2015**, *7*, 673−678.
(33) Kim, S.; Jin, S. H.; Lim, H. G.; et al. Synthetic cellular communication-based screening for strains with improved 3-hydroxypropionic acid secretion. *Lab Chip* **2021**, *21*, 4455−4463.
(34) Saleski, T. E.; Kerner, A. R.; Chung, M. T.; et al. Syntrophic co-culture amplification of production phenotype for high-throughput screening of microbial strain libraries. *Metab. Eng.* **2019**, *54*, 232−243.
(35) Saleski, T. E.; Chung, M. T.; Carruthers, D. N.; et al. Optimized gene expression from bacterial chromosome by high-throughput integration and screening. *Sci. Adv.* **2021**, *7*, No. eabe1767.
(36) Voyvodic, P. L.; Bonnet, J. Cell-free biosensors for biomedical applications. *Curr. Opin. Biomed. Eng.* **2020**, *13*, 9−15.
(37) Gräwe, A.; Dreyer, A.; Vornholt, T.; et al. A paper-based, cell-free biosensor system for the detection of heavy metals and date rape drugs. *PLoS One* **2019**, *14*, No. e0210940.
(38) Voyvodic, P. L.; Pandi, A.; Koch, M.; et al. Plug-and-play metabolic transducers expand the chemical detection space of cell-free biosensors. *Nat. Commun.* **2019**, *10*, No. 1697.
(39) Kieser, T.; Bibb, M. J.; Buttner, M. J.; Chater, K. F.; Hopwood, D. A. *Practical Streptomyces Genetics*; The John Innes Foundation Press: Norwich, 2000.
(40) Zou, X.; Hang, H. F.; Chen, C. F.; et al. Application of oxygen uptake rate and response surface methodology for erythromycin production by *Saccharopolyspora erythraea*. *J. Ind. Microbiol. Biotechnol.* **2008**, *35*, 1637−1642.
(41) Zou, X.; Hang, H. F.; Chu, J.; Zhuang, Y. P.; Zhang, S. L. Oxygen uptake rate optimization with nitrogen regulation for erythromycin production and scale-up from 50 L to 372 m^3 scale. *Bioresour. Technol.* **2009**, *100*, 1406−1412.

https://doi.org/10.1021/acssynbio.2c00102
ACS Synth. Biol. 2022, 11, 2697−2708